Indian Journal of Pure & Applied Physics
Vol. 48, August 2010, pp. 593-599

Multiferroic $Pb_{1-x}Sr_x(Fe_{0.012}Ti_{0.988})O_3$ nanoparticles: Room temperature dielectric relaxation, ferroelectricity and ferromagnetism

Kuldeep Chand Verma[1,2]*, Mast Ram[1], R K Kotnala[3], S S Bhatt[4] & N S Negi[1]

[1]Department of Physics, Himachal Pradesh University, Shimla 171 005, India

[2]Department of Physics, Eternal University, Baru Sahib, (H.P.), India

[3]National Physical Laboratory, New Delhi 110 012, India

[4]Department of Chemistry, Himachal Pradesh University, Shimla 171 005, India

*E-mail: kuldeep0309@yahoo.co.in

Rescived 25 March 2009; revised 18 February 2010; accepted 14 May 2010

The effect of particles size and lattice parameters on dielectric constant, ferroelectricity, ferromagnetism and *dc* resistivity of $Pb_{1-x}Sr_x(Fe_{0.012}Ti_{0.988})O_3$ (PSFT) nanoparticles has been studied at room temperature. The PSFT nanoparticles were prepared by a chemical synthesis route. The X-ray diffraction patterns confirm the phase structure of PSFT nanoparticles. The tetragonal distortion (*c/a*) and particles size have been reduced with increasing Sr^{2+} ion substitution. The microstructural behaviour shows the average particle's size of PSFT specimens which lie in the range of 4-13 nm. The Sr-doped PSFT specimens show higher value of dielectric constant than undoped PFT. At 30 mol% of Sr concentration, the PSFT specimen shows dielectric relaxation up to 18 MHz with $\varepsilon = 101$ and $\tan\delta = 0.075$. Also, the maximum value of saturation magnetization, $M_s = 64.4\times10^{-3}$ emu/g with low magnetic coercive field, $H_c = 35.9$ Oe, and spontaneous polarization, $P_s = 20.7$ μC/cm^2, remanent polarization, $P_r = 13.3$ μC/cm^2 and electric coercive field, $E_c = 5.7$ kV/cm have been observed. Compositional plots between average particle's size and *dc* resistivity, and dielectric constant and saturation magnetization have been given.

Keywords: Nanostructures, Chemical synthesis, Electron microscopy, Electrical properties, Magnetic properties

1 Introduction

Recently there is an increasing interest in coexistence of the ferroelectricity and ferromagnetism of multiferroics has wide range of new applications including spintronics[1], new data-storage media[2] and multiple-state memories[3]. Ferromagnetism and ferroelectricity originate from local spins and off-center structural distortion, respectively. Ferromagnetism and ferroelectricity are two quite unrelated phenomenons, but coexists in certain unusual materials called multiferroics or magnetoelectrics[4,5]. Such multiferroics are rare in nature or not widely synthesized in laboratory and also possess simultaneously magnetic and dielectric polarization called magnetoelectric coupling usually much below or above room temperature[6-8]. This scarcity of multiferroic materials creates a major limitation to understand the physics of coupling between magnetic and electric parameters. Therefore increasing attention has more focus on the synthesis of new multiferroic materials which results in magnetic and electric coexistence and coupling at room temperature. There are three direct approaches have been used to synthesize a new multiferroic material. The first one is the multiferroic composite made by ferroelectrics and ferromagnetic heterostructure. The second involves preparation of super lattices composed of ferroelectric and ferromagnetic layers alternatively, where symmetry breaking may induce ferroelectricity and ferromagnetism. The third approach deals with doping of transition metals (i.e., Fe, Co, Ni, W, etc.) in Bi and perovskite (ABO_3) based compounds. Survey of literature has found limitations in Bi based multiferroic systems due to their low resistivity value and non stoichiometric behaviour. So, a few studies have focus on inducing coexistence of ferromagnetism and ferroelectricity at room temperature and have presented a promising potential in recent multiferroic based technology. Among them, Palkar *et al.*[9] first observed magnetoelectric behaviour in bulk ferroelectric $PbTiO_3$ by partially substituting Ti with Fe. They have also reported the similar properties in thin film form of the same system[10]. Ren *et al.*[11] reported room temperature ferro-magnetism in Fe-doped $PbTiO_3$ nanocrystals, and

prepared these by a chemical synthesis route using polyethylene glycol (PEG) as surfactant. We have recently synthesized the Fe-doped $PbTiO_3$ (PFT) nanoparticles by chemical route and used polyvinyl alcohol (PVA) as surfactant which acts more efficient than PEG in reducing the particles size[12]. These PFT nanoparticles with 1.2 mol% of Fe concentration showed strong ferromagnetism (M_s = 41.6 × 10^{-3} emu/g), but small value of dielectric constant. In our more recent report[13], the 30 mol% of Sr substitution in a similar composition of $Pb(Fe_{0.012}Ti_{0.988})$ (PSFT3) has further reduced the particles size into few nanometer. The observed ferromagnetism was also strong with large value of electrical polarization. So, it is important to study PSFT system with varying Sr concentrations and find the resulted values of lattice parameters, particles size, *dc* resistivity, dielectric constant, spontaneous polarization and ferromagnetism.

In the present work, we have investigated the effect of Sr doping in $Pb_{1-x}Sr_x(Fe_{0.012}Ti_{0.988})O_3$ (PSFT) system [x = 0.1 (PSFT1), 0.2 (PSFT2), 0.3 (PSFT3) and 0.4 (PSFT4)] on the structural, dielectric, electrical and magnetic properties.

2 Experimental Details

The PSFT nanoparticles were prepared by a chemical synthesis route using polyvinyl alcohol (PVA) as a surfactant. The precursor solution was synthesized from lead acetate, strontium acetate, tetra-n-butyl orthotitanate and ferric chloride. The preparation of PFT nanoparticles was described in our previous work[12]. We have employed requisite amount of Sr compound to the precursor solution to prepare PSFT nanoparticles of various composition. The ultimate mixture appeared as a clear gel at room temperature. The gel has been dried at 300°C and annealed at 700°C for 2h to crystallize the specimens. The structural phase identification was carried out by X-Ray Diffraction (XRD) using PANalytical's X-Pert PRO system. The nanostructural analysis of PSFT particles were carried out by Transmission Electron Microscopy (TEM) using Hitachi H-7500 system and Scanning Electron Microscopy (SEM) using JEOL JSM6100 system. For TEM measurements, distilled water has been used as a solvent in which the PSFT powders were dissolved. Magnetic measurements were performed on PSFT powder specimens at room temperature by using Vibrating Sample Magnetometer (VSM-735). For electrical measurements (i.e., dielectric constant, spontaneous polarization, *dc* resistivity, etc.), the annealed powder was pressed into pellets of thickness ~ 0.5 mm by the cold isotatic pressing method with a pressure of 5 bar for 10 min and then sintered at 1000°C for 5h. The density of pellet specimens was obtained using Archimedes method which improved up to 8.1 gcm^{-3} (96%) of theoretical density for perovskite $PbTiO_3$ (8.42 g cm^{-3}). The dielectric properties of the specimens were examined using an Agilent 4285A LCR meter. The *dc* resistivity was measured at room temperature by using Keithley 2611 source meter. The spontaneous polarization was carried out on poled pellet specimens by using *PE* loop Tracer of MARINE INDIA ELECT. For these measurements, Ag contact was deposited on both the surface of pellet as top and bottom electrodes.

3 Results and Discussion

The XRD patterns of the PSFT nanoparticles annealed at 700°C are shown in Fig. 1. It is evident from XRD that a single perovskite phase exists in all the specimens except some minor impurity peaks of pyrochlore ($Pb_2Ti_2O_6$) phases in PSFT1 and PSFT4. The similar impurity peaks are also observed in $Pb(Fe,Ti)O_3$ system by Palkar *et al*[9]. With increasing

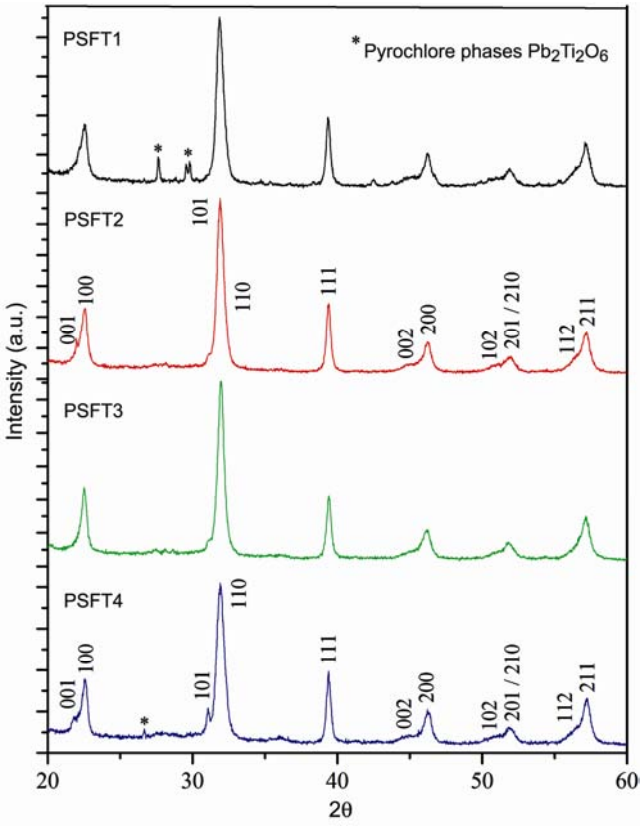

Fig. 1—XRD pattern of PSFT nanoparticles heated at 700°C for 2h with diffraction angle (2θ) varies from 20-60°

Sr concentration in PFT, the similar ionic environment of Sr^{2+} and Pb^{2+} ions causes hopping mechanism between these intrinsically without via oxygen vacancies and resulting into decrease in oxygen vacancies (V_O). Thus, PSFT1 shows small intensity of impurity peaks, and PSFT2 and PSFT3 specimens are free from these peaks. However, PSFT4 shows minor impurity peak due to excess of Sr^{2+} ions towards Pb^{2+} causes possibility of hopping via oxygen. The crystalline structure revealed that the PSFT nanoparticles exhibit same structure of parent $PbTiO_3$. The splitting of (001)/(100) and (101)/(110) peaks of $PbTiO_3$ represent a tetragonal phase. With increasing Sr concentration, the peaks slightly shifted towards higher angles. According to the (101)/(110) doublets, tetragonal structures has been formed in PSFT1, PSFT2, PSFT3 and PSFT4 nanoparticles. However, a strong overlapping was also observed in PSFT2 and PSFT3 nanoparticles, shows low degree of tetragonal distortion. This indicates that the structure changes from tetragonal to pseudo-cubic phase. With Sr-doping, the peaks (101)/(110) greatly shifted towards higher angles when compared with pure PFT system[12]. On further increasing Sr up to 30 mol%, a slight increase in the peak intensity is seen. In case of PSFT4, the peaks shifted toward lower angles with less intensity of (101) peak than (110). This type of crystalline behaviour exists at higher Sr concentration and reported in the literature[14]. The tetragonal (*c*/*a*) ratio of PSFT nanoparticles was highly reduced (i.e., values of *c*/*a* have been reduced from 1.0046 to 1.0032) with Sr doping and compared it with parent $PbTiO_3$ (1.066)[15]. However, PSFT4 specimen shows anomaly in *c*/*a* ratio than other PSFT specimens. This anomaly in *c*/*a* may be due to apposing nature of the splitting of (101)/(110) peaks for PSFT4. The values of *c*/*a* ratio of PSFT nanoparticles are given in Table 1. Also, we see all diffraction peaks as the characteristic of $PbTiO_3$ were shifted upward with increasing Sr concentration. This may be due to the lattice contraction of Sr replaces Pb with a slightly smaller ionic radius of Sr^{2+} than Pb^{2+} ion.

The average particle's size of PSFT specimens was calculated from $\Delta 2\theta_{1/2}$ using Scherer's relation [16]. The values of average particle's size have been reduced from 13±2 to 4±1 nm with increasing Sr concentration and are given in Table 1. These calculated values are quite smaller than reported 24 nm for pure PFT specimen [12] was prepared by a similar chemical route. Such significant reduction in the particle's size of PSFT specimens may be due to the doping of Sr and the effect was reported in $Pb_{0.8}Sr_{0.2}TiO_3$ system [17]. The nanostructural behaviour of PSFT nanoparticles was also confirmed from their micrographs. Figs 2(a) and 2(b) shows the TEM images of PSFT2 and PSFT3 specimens and the SEM image of PSFT3 was also given in Fig. 2(c). From TEM analysis, the average value of particle's size is measured as 10 ± 1 nm for PSFT2 and 7 ± 1 nm for PSFT3 specimens. In TEM images each particle can be seen widely distributed due to suspension of particles in the solvent during measurements. Using statistical analysis in SEM image, the average value of particle's size is measured as 9 ± 1 nm for PSFT3 specimen. These measured values of average particle's size from micrographs are consistent with that calculated by XRD peaks.

The dielectric properties of PSFT nanoparticles with varying Sr concentration are shown in Fig. 3. The dispersionless dielectric response at lower frequency is observed. Most of the dielectric materials found in the literature[18,19] have shown dielectric dispersion at lower frequency. This dispersion may be attributed to the dipoles resulting from changes in volume states of cations and space charge polarization. The loss tangent of all the PSFT specimens was below 0.06 and the dielectric constant (ε) increased greatly with 10 mol% of Sr concentration in PFT system. For pure PFT system, the observed value of dielectric constant is 48[12]. However, the observed value of ε for PSFT1, PSFT2, PSFT3 and PSFT4 specimens are 125, 96, 83 and 79, respectively, at frequency of 1 MHz. The phenomenon is due to the tendency of decreasing Curie temperature (T_c) towards room temperature as

Table 1 — Properties of PSFT nanoparticles

Composition	*c*/*a* ratio	Particle's size (nm)	ε at 1 MHz	ε at 18 MHz	*dc* resistivity (ρ_{dc}) (10^{11} Ωcm)
PSFT1	1.0046	13 ± 2	125	Resonance	0.369
PSFT2	1.0041	11± 0.5	96	Resonance	3.289
PSFT3	1.0032	8 ± 1	83	101	3.619
PSFT4	1.0037	4 ± 1	79	100	4.243

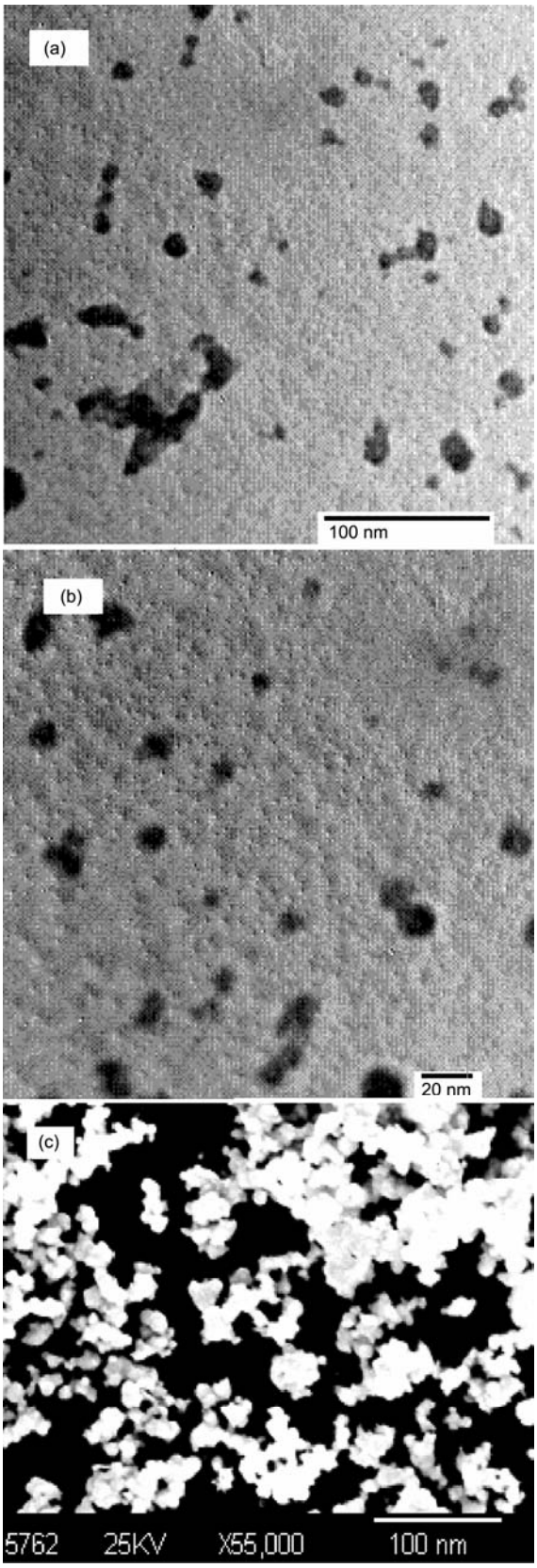

Fig. 2—TEM of (a) PSFT2, (b) PSFT3, and (c) SEM of PSFT3, specimens

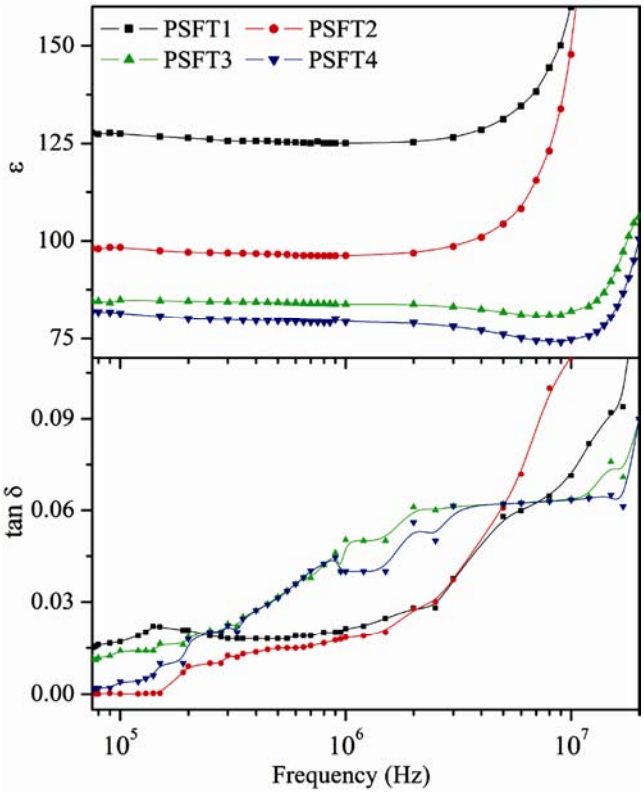

Fig. 3—The variation of dielectric constant (ε) and tanδ with frequency

increasing the Sr concentration[20]. Because the Curie temperature of $PbTiO_3$ is 763 K and that of $SrTiO_3$ is 20 K (Ref. 21). Also a slight reduction in the value of dielectric constant is observed when the Sr concentration was increased above 10 mol%. This reduction may be due to decrease in the value of average particle's size with increasing Sr concentration in the PSFT specimens. Since the specimens with smaller grain sizes contain a relatively larger volume fraction of grain boundary atoms in between the grains. These boundaries act as a barrier for current conduction between grains, resulting in an increase of *dc* resistivity of the specimen. The higher resistivity of smaller grains increases the threshold fields, which results into lower value of dielectric constant but shows stable dielectric relaxation up to higher frequency region. The values of *dc* resistivity with different Sr concentration in PSFT specimens are given in Table 1. Lichtensteiger *et al.*[22] studied ferroelectric and tetragonal behaviour of $PbTiO_3$ and reported the smaller value of tetragonal distortion (*c*/*a*) which can highly suppressed the electrical polarization resulting into stable polarization signal. Because the electric dipoles in this case are formed with uniform alignments and creates difficulty during

electrical polarization. In the present PSFT specimens, the values of *c*/*a* ratio have been reduced with increasing Sr concentration and involve another reason for smaller values of dielectric constant with increasing Sr concentration. The dielectric relaxor behaviour is observed up to higher frequency in all the PSFT specimens. As the particles size decreased, the dielectric relaxation is increases towards higher frequency and vice versa. This relaxation in dielectric constant has been observed up to 8 MHz for PSFT1, 10 MHz for PSFT2, 17 MHz for PSFT3 and 18 MHz for PSFT4 specimens, respectively. The values of dielectric constant in all the PSFT specimens at frequencies of 1 and 18 MHz are given in Table 1. Such dielectric relaxation at higher frequency may be due to higher values of *dc* resistivity of PSFT nanoparticles. The upward trend in the values of dielectric constant at higher frequencies is due to resonance effect[23]. The low losses are observed in all PSFT specimens and involve a similar explanation like dielectric constant as discussed above. The dielectric loss slightly increases at higher frequency due to the influence of contact resistance between specimen and electrode.

The strong ferromagnetic behaviour like PFT system is also observed in all the PSFT nanoparticles

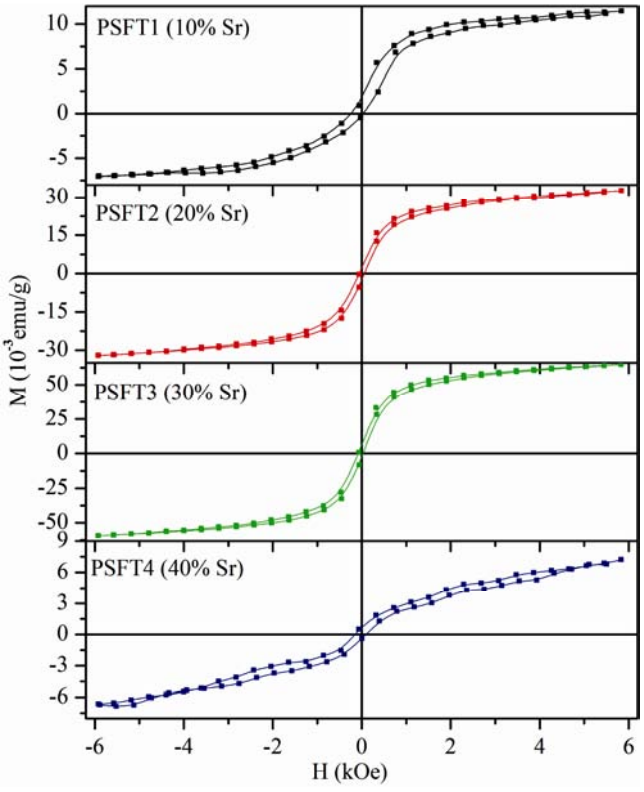

Fig. 4—Magnetization (*M*) versus magnetizing field (*H*) curves of PSFT specimens

specimens as shown in Fig. 4. The values of saturation magnetization (M_s) were slightly small in case of PSFT1 and PSFT2, and slightly large in PSFT3 than pure PFT system. However, the value of remanent magnetization is observed as same in PFT and all PSFT specimens. It is also observed that the value of coercive field (H_c) is reduced with the doping of Sr which makes clear *S*-type hysteresis loop and indicates the improvement in ferromagnetism of these PSFT specimens. It can be clearly seen that the specimens up to 30 mol% of Sr, *S*-shaped hysteresis loops are observed, which indicate the ferro-magnetism of PSFT nanoparticles. However, the PSFT4 specimen has show weak ferromagnetism. In other wards, magnetic studies indicate that the ferromagnetic ordering increased with $x \leq 0.3$. This increase of ferromagnetic ordering on increasing Sr concentration may be due to decrease in the particles size. Since small particles size has less contribution to the superparamagnetic relaxation[24]. The weak ferromagnetic behaviour at $x = 0.4$ may probably due to the influence of higher Sr concentration on *F*-center exchange mechanism in Fe^{3+}-V_O^{2-}-Fe^{3+} groups, which dominates the particles size effect. We have observed $M_s = 64.4 \times 10^{-3}$ emu/g and $H_c \sim 35$ Oe for PSFT3 specimen. The values of M_s and H_c for all the PSFT specimens are given in Table 2. It is noticed that the observed ferromagnetism shows improvement than our previous reported PFT system and other nano multiferroic systems[18,25], and non magnetic nanoparticles[26] of $BaTiO_3$. In the view of ref. 26, it is believed that there is little contribution in ferromagnetism of non magnetic nanoparticles which arises from magnetic moments of oxygen vacancies on the surface of the nanoparticles, i.e., point defects such as cation and anion vacancies in insulator can create magnetic moments.

Polarization hysteresis measurements at room temperature were performed at different frequencies of 50, 100, 300 and 400 Hz. The hysteresis loops as a function of Sr content are as shown in Fig. 5. All the PSFT specimens show saturated ferroelectric loops.

Table 2 — Ferromagnetic and ferroelectric properties of PSFT nanoparticles

Composition	M_s (10^{-3}emu/g)	H_c (Oe)	P_s (μC/cm^2)	P_r (μC/cm^2)	E_c (kV/cm)
PSFT1	11.0	298.0	16.68	11.57	6.16
PSFT2	31.1	56.15	18.05	12.2	5.9
PSFT3	64.4	35.9	20.7	13.3	5.7
PSFT4	6.2	98.0	10.2	5.0	6.12

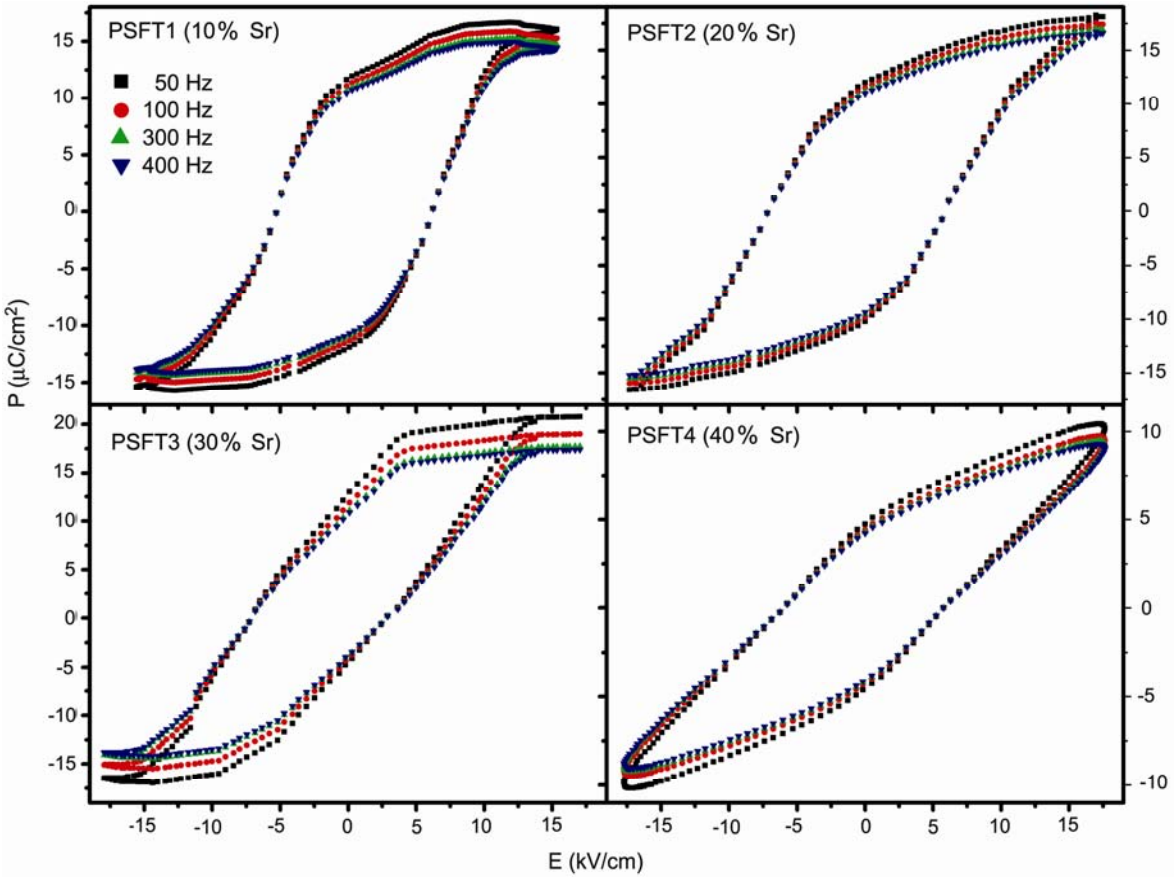

Fig. 5 — Polarizations versus applied voltage hysteresis loops measured at different frequencies

Figures 4 and 5 demonstrate good coexistence of ferromagnetic and ferroelectric behaviours at room temperature for Sr substituted PFT nanoparticles. With increasing Sr concentration, the spontaneous polarization, P_s and remanent polarization, P_r is increased, and at 50 Hz the observed values of P_s, P_r and coercive field (E_c) are illustrated in Table 2. The maximum value of electrical polarization observed in PSFT3 specimen (i.e., the values of P_s, P_r and E_c at 50 Hz are 20.7 μC/cm^2, 13.3 μC/cm^2 and 5.7 kV/cm, respectively) than other PSFT specimens with 10, 20 mol% of Sr concentration. The improvement in these ferroelectric properties may be due to combined effect related to decrease in their dielectric anisotropy (lower *c*/*a* ratio) and reduction in the particles size. The weak ferroelectric response in PSFT4 specimen arises due to presence of impurity phase. Also with increasing frequency, each *P*-*E* loop of PSFT specimens shows more ferroelectric switching behaviour.

The effect of Sr concentration in PFT system on the particles size, *dc* resistivity, dielectric constant and saturation magnetization is shown in Fig. 6. The

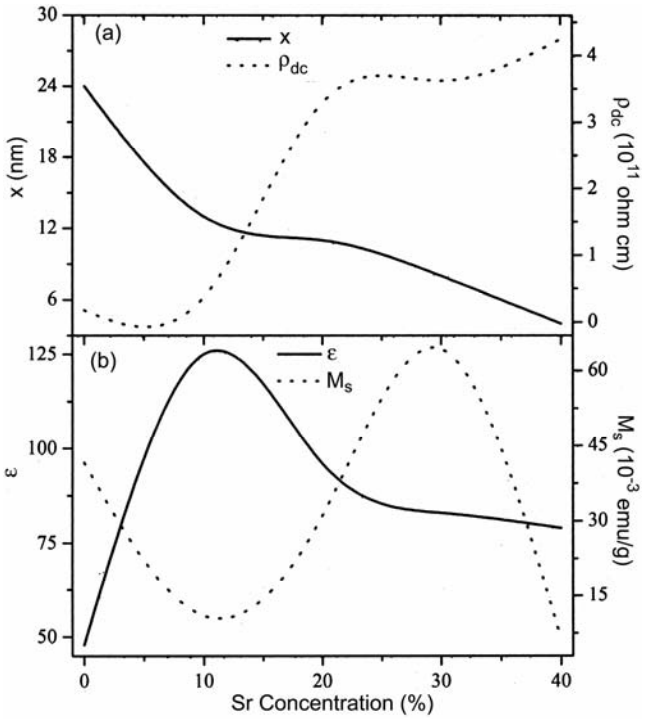

Fig. 6 — Compositional data of PSFT specimens

values of these parameters at zero Sr concentration are also taken from our previous reported work[12]. Fig. 6(a) shows increment in the value of *dc* resistivity with decreasing particles size of PSFT specimens with increasing Sr concentration in PSFT system. The higher value of *dc* resistivity in the order of 10^{11} Ωcm has been observed. This higher value of *dc* resistivity is indicated that the PSFT specimens involve transport mechanism of electrons due to indirect band conduction mechanism and only by defect states in the Fermi gap[27]. The corresponding behaviours of dielectric constant and saturation magnetization are shown in Fig. 6(b). It can be seen that the value of dielectric constant increased rapidly with small relaxation at low Sr concentrations. At higher Sr concentrations, the relaxation remains stable and consistent with the *dc* resistivity curve. According to Devonshire-Ginzburg-Landau (DGL) theory[22], the reduction in the structural parameters such as particles size, *c*/*a* ratio etc. of ferroelectric material results into the suppression of electrical polarization and gives stable dielectric relaxation. A similar explanation may also holds in the magnetization curve. Hence, the PSFT2 and PSFT3 specimens exhibit good ferroelectric and ferromagnetic coexistence at room temperature[28,29].

4 Conclusions

In conclusion, PSFT nanoparticles were synthesized by chemical route using PVA as a surfactant. The structural, electrical and magnetic properties were investigated to examine the influence of the Sr concentration. The XRD pattern shows that the values of average particle's size and *c*/*a* ratio are decreased with increasing the Sr concentration. The TEM and SEM measurements were also confirms the nanostructural behaviour of PSFT specimens. The PSFT specimens show higher value of *dc* resistivity in the order of 10^{11} Ωcm and dispersionless dielectric properties up to a higher frequency region of 18 MHz. One important conclusion of this work is that the good coexistence of ferromagnetism and ferroelectricity at room temperature occurs in a stable perovskite structure of these PSFT nanoparticles. Among the PSFT specimens, 30 mol% Sr concentrations show highest value of $M_s \sim 64.4 \times 10^{-3}$ emu/g and good ferroelectric properties with $P_s \sim 20.7$ μC/cm^2, $P_r \sim 13.3$ μC/cm^2 and $E_c \sim 5.7$ kV/cm.

References

1 Fiebig M, Lottermoser T, Frohlich D, Goltsev A V & Pisarev R V, *Nature,* 419 (2002) 818.
2 Spaldin N A & Fiebig M, *Science,* 309 (2005) 391.
3 Hill N A, *J. Phys Chem B,* 104 (2000) 6694.
4 Hemberger J, Lunkenheimer P, Fichtl R, Krugvon N H A, Tsurkan V & Loidl A, *Nature,* 434 (2005) 364.
5 Eerenstein W, Mathur N D & Scott J F, *Nature*, 442 (2006) 759.
6 Yamasaki Y, Miyasaka S, Kaneko Y, He J P, Arima T & Tokura Y, *Phy. Rev Lett,* 96 (2006) 207204.
7 Gajek M, Bibes M, Fusil S, Bouzehouane K, Fontcuberta J, Barthelemy A & Fert A, *Nat Mater,* 6 (2007) 296.
8 Kumar S, Kumar R, Dogra A, Reddy VR, Banerjee A & Alimuddin, *Indian J. Pure Appl Phys,* 45 (2007) 31.
9 Palkar V R & Malik S K, *Solid State Commun* 134 (2005) 783.
10 Palkar V R, Purandare S C, Gohil S, John J & Bhattacharya S, *Appl Phys Lett,* 90 (2007) 172901.
11 Ren Z, Xu G, Wei X, Liu Y, Hou X, Du P, Wang W, Shen G & Han G, *Appl Phys Lett,* 91 (2007) 063106.
12 Verma K C, Kotnala R K & Negi N S, *Appl Phys Lett,* 92 (2008) 152902.
13 Verma K C, Singh M, Kotnala R K & Negi N S, *Appl Phys Lett,* 93 (2008) 072904.
14 Thomas R, D. C. Dube, M. N. Kamalasanan, S. Chandra, A.S. Bhalla, *J Appl Phys*, **82**, 4484(1997).
15 Chu S Y & Chen C H, *Sensors and Actuators A,* 89 (2001) 210.
16 Cullity B D, *X-ray Diffraction* (Addision-Wesley, Reading, MA), 1967.
17 Verma K C, Kotnala R K, Mathpal M C, Thakur N, Gautam P & Negi N S, *Mater Chem & Phys,* 114 (2009) 576.
18 Kumar A, Rivera I, Katiyar R S & Scott J F, *Appl Phys Lett,* 92 (2008) 132913.
19 Devan R S, Dhakras D R, Vichare T G, Joshi A S, Jigajeni S R, Ma Y R & Chougule B K *J Phys D: Appl Phys,* 41 (2008)105010.
20 Chen H Y, Wu J M, Huang H E & Bor H Y, *J Crystal Growth,* 308 (2007) 213.
21 Ziese A, Vrejoiu I, Setzer A, Lotnyk A & Hesse D, *N J Phys,* 10 (2008) 063024.
22 Lichtensteiger C, Triscone J M, Junquera J & Ghosez P, *Phys Rev Lett,* 94 (2005) 047603.
23 Kapustianyk V, Shchur Y, Kityk I, Rudyk V, Lach G, Laskowski L, Tkaczyk S, Swiatek J & Davydov V, *J Phys Condens Matter,* 20 (2008) 365215.
24 Roy M K, Haldar B & Verma H C, Nanotechnology 17 (2006) 232.
25 Cho J H, Hwang T J, Joh Y G, Kim E C, Kim D H, Lee K J, Park H W, Ri H C, Kim J P & Cho C R, *Appl Phys Lett,* 88 (2006) 092505.
26 Mangalam R V K, Ray N, Waghmare U V, Sundaresan A & Rao C N R, *Solid State Commun,* 149 (2009) 1.
27 Verma K C, Thakur N, Kotnala R K & Negi N S, *J Phys D,* 41 (2008) 215108.
28 Kukreti A, Kumar A & Naithani U C, *Indian J Pure Appl Phys*, 46 (2008) 276.
29 Upadhyay T C & Semwal K P, *Indian J Pure Appl Phys*, 47 (2009) 883.